DNA/RNA Nanotechnology Hot Paper

International Edition: DOI: 10.1002/anie.201508978
German Edition: DOI: 10.1002/ange.201508978

A Multi-RNAi Microsponge Platform for Simultaneous Controlled Delivery of Multiple Small Interfering RNAs

*Young Hoon Roh, Jason Z. Deng, Erik C. Dreaden, Jae Hyon Park, Dong Soo Yun, Kevin E. Shopsowitz, and Paula T. Hammond**

Abstract: *Packaging multiple small interfering RNA (siRNA) molecules into nanostructures at precisely defined ratios is a powerful delivery strategy for effective RNA interference (RNAi) therapy. We present a novel RNA nanotechnology based approach to produce multiple components of polymerized siRNA molecules that are simultaneously self-assembled and densely packaged into composite sponge-like porous microstructures (Multi-RNAi-MSs) by rolling circle transcription. The Multi-RNAi-MSs were designed to contain a combination of multiple polymeric siRNA molecules with precisely controlled stoichiometry within a singular microstructure by manipulating the types and ratios of the circular DNA templates. The Multi-RNAi-MSs were converted into nanosized complexes by polyelectrolyte condensation to manipulate their physicochemical properties (size, shape, and surface charge) for favorable delivery, while maintaining the multifunctional properties of the siRNAs for combined therapeutic effects. These Multi-RNAi-MS systems have great potential in RNAi-mediated biomedical applications, for example, for the treatment of cancer, genetic disorders, and viral infections.*

Key aspects of RNA nanotechnology[1] rely on the functional diversities of RNA molecules (e.g., gene silencing, catalytic activity, and regulatory roles) and their structural complexities (e.g., secondary structure motifs and loops).[2] These properties of RNAs as biologically functional nanomaterials enable the construction of RNA-based nanostructures for numerous biological and therapeutic applications.[3] Furthermore, RNA interference (RNAi) based therapy using small interfering RNA (siRNA) has been intensely investigated as a powerful approach for therapeutic applications, including cancer treatment, because of its unique capacity for achieving sequence-specific gene silencing.[4] By combining structural RNA nanotechnology and RNAi, we recently developed a self-organized RNAi delivery approach based on the self-assembly of highly concentrated and polymerized siRNA into sponge-like porous magnesium pyrophosphate microstructures (RNAi-MSs).[5,6] To enhance both intracellular and systemic delivery of polymeric nucleic acids, modification of the microsponge structure can be achieved in two steps: 1) condensation of the microsponge structures into nanostructure complexes, and 2) progressive electrostatic layer-by-layer (LbL) adsorption of various biomaterials onto the condensed nanoparticles.[7]

Building on these previous findings, the next critical challenge with this delivery system was to expand the versatility and practicality of delivering RNAi molecules for potent therapeutic efficacy. Several disorders and clinical conditions are the result of genetic dysregulation, often impacted by multiple gene pathways that can be highly interdependent. To achieve synergistic and effective therapies based on RNAi, the simultaneous controlled release of multiple siRNAs may be required, and in many cases, the relative amounts and/or timeframes of suppression can require precision approaches towards delivery.[4,8] A promising approach would be to stably, safely, and effectively deliver large quantities of multiple RNAi molecules into targeted tumors in a controlled manner.[9] To address these critical issues, we herein report a modular platform for synthesizing multiple components of polymeric RNAi molecules that self-assemble into microsponge structures (Multi-RNAi-MSs) by rolling circle transcription (RCT). The types and ratios of multiple polymeric RNAi molecules within individual RNAi microsponge structures are easily manipulated depending on the circular DNA template design and fine-tuning of the reaction conditions at the RCT stage. These packaged multiple polymeric RNAi molecules can be further assembled into nanoparticles by a condensation step, leading to favorable physicochemical properties for efficient cellular uptake. As a result, the Multi-RNAi-MS method represents a means of producing well-controlled, multifunctional, biocompatible, polymeric RNAi molecules designed for the simultaneous silencing of genes, both in terms of packaging and delivery efficacy.

To generate microsponges containing multiple types of polymeric RNAi molecules, we first designed linear DNA template sequences (Table S1) and then constructed a circular DNA library. Each linear single-stranded DNA (ssDNA) template was comprised of complementary sense and anti-

[*] Prof. Y. H. Roh, Dr. J. Z. Deng, Dr. E. C. Dreaden, Dr. D. S. Yun, Dr. K. E. Shopsowitz, Prof. P. T. Hammond
Department of Chemical Engineering
Massachusetts Institute of Technology
Cambridge, MA 02139 (USA)
and
Koch Institute for Integrative Cancer Research at MIT
Cambridge, MA 02139 (USA)
E-mail: hammond@mit.edu
Prof. Y. H. Roh, J. H. Park
Department of Biotechnology, Yonsei University
Seoul, 120-749 (Republic of Korea)

Supporting information for this article is available on the WWW under http://dx.doi.org/10.1002/anie.201508978.

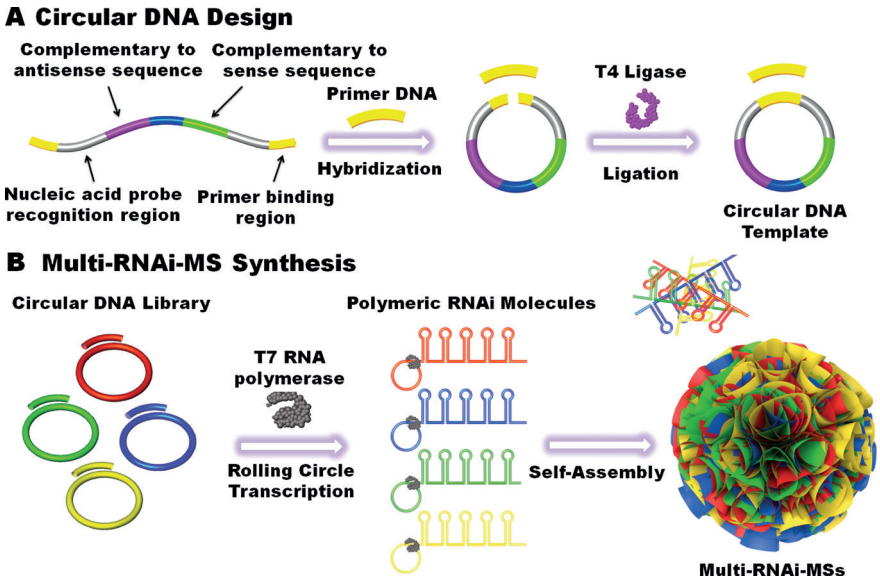

Figure 1. Design and synthesis of multiple-component RNAi microsponges (Multi-RNAi-MSs). A, B) Synthesis of Multi-RNAi-MSs with different types of circular DNA. A circular DNA library was constructed using individual circular DNA templates that encode each siRNA sequence. Numerous combinations of circular DNAs can be used to generate Multi-RNAi-MSs, depending on the application intended.

sense siRNA sequences, spacer regions, molecular-probe recognition sites, and primer-binding sites (Figure 1 A). As a proof of concept to test the different siRNA functions of multiple polymeric RNAi molecules, the siRNAs were designed with complementary sense and antisense sequences corresponding to two different reporter genes [i.e., green fluorescent protein (GFP) and red fluorescent protein (RFP)]. The various circular DNAs used to construct the modular library of polymeric RNAi molecules were synthesized by hybridizing linear DNAs to complementary primers and performing enzymatic ligations. Gel electrophoresis was conducted to confirm the generation of circular DNA structures from these hybridized and ligated linear strands. Band shifts reflecting the conversion of linear DNAs into circular DNAs were observed, demonstrating the successful generation of a circular DNA library (Supporting Information, Figure S1). By using predefined sets of circular DNAs during RCT, multiple functional types of polymeric RNAi molecules were simultaneously generated, which could then self-assemble to form Multi-RNAi-MSs (Figure 1 B).

After purification to obtain well-dispersed Multi-RNAi-MSs, the morphologies and structures of the Multi-RNAi-MSs (with the GFP and RFP polymeric RNAi molecules in a ratio of 1:1) were investigated by scanning electron microscopy (SEM), confocal microscopy, and transmission electron microscopy (TEM). The SEM image shows that the Multi-RNAi-MSs were spherical in shape and uniformly micrometer-sized composite particles (ca. 1 μm diameter) with a sponge-like surface porosity (Figure 2 A). The morphological characteristics of the Multi-RNAi-MSs were further studied by confocal microscopy to observe the presence and distribution of the multiple polymeric RNAi molecules in the microsponges. For this approach, we used Cy5-UTP labeling during the RCT process, yielding polymeric RNAi molecules with red fluorescence (Figure 2 B). The red fluorescence in the confocal microscopy image indicated that the polymeric RNA transcripts were distributed fairly evenly throughout the particles, which consist of the polymeric transcripts bound to crystalline magnesium pyrophosphate scaffolds. Furthermore, the TEM image showed that the structures of the Multi-RNAi-MSs comprise highly compact, multilayered thin sheets that branch hierarchically outwards from a dense inner core (Figure 2 C and Figure S2). The Multi-RNAi-MSs were further analyzed by cryo-TEM to determine their complex structures in a native environment without dehydration (Figure 2 D). The cryo-TEM image more clearly shows the extensive nanocrystalline structure of the particles, and suggests a large internal surface area within the sheet-like crystals.

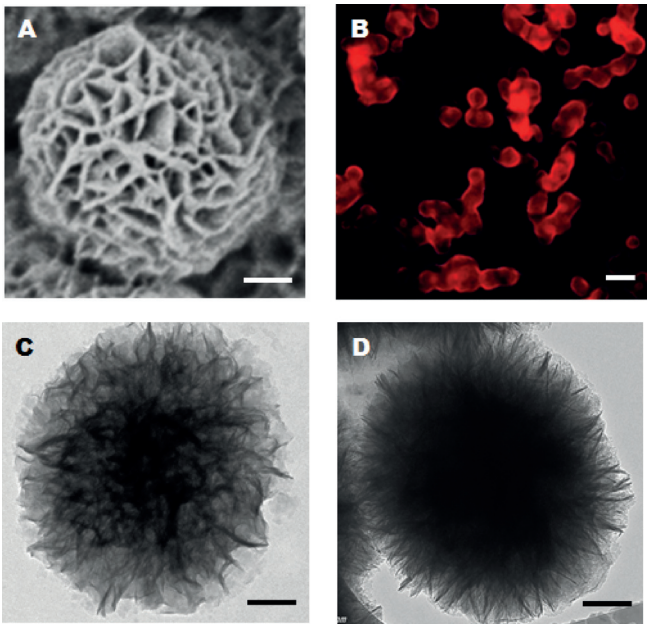

Figure 2. Characterization of the Multi-RNAi-MSs. A) SEM image of a Multi-RNAi-MS. Scale bar: 1 μm. B) Confocal microscopy image of Multi-RNAi-MSs that had been functionalized with Cy5-conjugated dUTP during the RCT process (red). The Multi-RNAi-MSs are shown in the middle section. Scale bar: 1 μm. C, D) TEM and cryo-TEM images of Multi-RNAi-MSs at higher magnification. Scale bars: 200 nm.

It is important to note that this facile engineering approach for synthesizing Multi-RNAi-MSs can incorporate different ratios/combinations of multiple polymeric RNAi molecules to elicit various biological responses. The relative amounts of the different polymeric RNAi molecules that

were incorporated into the microsponges were easily manipulated by controlling the ratios of circular DNAs combined in the RCT reactions. Five types of Multi-RNAi-MSs were constructed by controlling the ratios of the RNA components. Their construction was based on varying the molar ratio of the two different circular DNA templates (4:1, 2:1, 1:1, 1:2, and 1:4) that were used for the RCT reactions. After the RCT process, two molecular probes [fluorescently tagged short oligonucleotides (ca. 20 bases) with green or red fluorescence] were hybridized to the pre-designed recognition sites encoded into each of the two polymeric RNAi molecules of the microsponges. This hybridization resulted in merged fluorescence signals whose relative component intensities depended on the molar ratio of the polymeric RNAi molecules generated within each Multi-RNAi-MS type. Therefore, different Multi-RNAi-MSs (4G1R, 2G1R, 1G1R, 1G2R, and 1G4R) could be decoded by determining the fluorescence intensity ratios between the sequence-specific probes. Confocal microscopy was utilized to confirm the presence of the two polymeric RNAi molecule components within individual microsponge structures by observing the merged fluorescence intensities. The fluorescence intensity ratio varied as a function of the ratio of the polymeric RNAi molecules incorporated into the Multi-RNAi-MSs (Figure 3A). In this manner, we confirmed that the expected and observed fluorescent intensity ratios of the Multi-RNAi-MSs were highly correlated, indicating the successful incorporation of polymeric RNAi molecules at the intended ratios

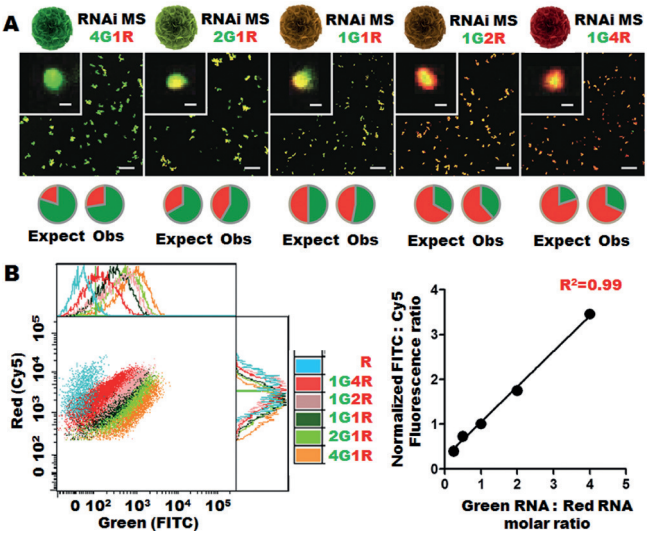

Figure 3. Characterization of Multi-RNAi-MSs obtained with the ratio control system. A) Confocal microscopy images of Multi-RNAi-MSs prepared according to the ratio control system. Five types of Multi-RNAi-MSs containing various amounts of polymeric RNAi molecules were synthesized by subjecting various combinations of circular DNA templates to RCT. The Multi-RNAi-MSs were hybridized with two fluorescent-dye-conjugated nucleic acid probes after the RCT process (yielding green or red fluorescence). Scale bars: 5 μm and 500 nm (inset). B) Flow cytometry analysis of the Multi-RNAi-MSs. The green channel indicates FITC and the red channel indicates APC. The R^2 value refers to the correlation between the observed green/red fluorescence intensity ratio and the pre-determined green/red polymeric RNAi molar ratio.

during the synthesis of the microsponge structures. The presence of multiple components within each singular RNAi microsponge structure was further confirmed by flow cytometry analysis. The ratio of the normalized intensities was calculated as I_R/I_G, where I_R and I_G are the red and green fluorescence intensities from both nucleic acid tags in the Multi-RNAi-MSs, respectively. These results also demonstrated the feasibility of precisely controlling the relative amounts of multiple components of polymeric RNAi molecules within Multi-RNAi-MSs by varying the ratio of the hybridized DNA templates (Figure 3B).

It is necessary to obtain RNAi particles with appropriate physicochemical properties, with respect to size, shape, and surface charge, especially for practical biological applications such as systemic drug delivery.[10] Our strategy for developing Multi-RNAi-MSs as a drug-delivery platform involved an additional condensation step by electrostatic interactions and physical agitation.[5–7] In this study, positively charged linear polyethylenimine (PEI) was chosen to achieve effective intracellular uptake and endosomal escape. We observed the additional packaging of polymeric RNAi molecules by PEI-induced condensation. Confocal microscopy images revealed that the size of the Multi-RNAi-MSs was reduced in the presence of PEI (1 mg mL^{-1}) after the condensation process (Figure 4A,B). We further examined the presence of multiple polymeric RNAi molecules in the condensed particles (Figure S3). The morphology and physical size of the condensed structures were further analyzed by TEM and compared with the structures of the original Multi-RNAi-MSs. We observed the formation of uniform polyplex structures, and the average particle size of the condensed particles was approximately 102 nm (Figure 4C and Figure S4). Furthermore, the size and surface charge of the Multi-RNAi-MSs before and after the condensation step were determined by dynamic light scattering (DLS) and zeta potential measurements, confirming the ability to reverse particle surface charge and the successful condensation of the Multi-RNAi-MSs with PEI (Figure S5). These results suggest that the Multi-RNAi-MSs were transformed in terms of their structural morphology, particle size, and surface charge by disruption of the negatively charged Multi-RNAi-MSs and subsequent complexation with a positively charged polymer. We refer to these highly compact, nanosized complex particle structures consisting of multiple polymeric RNAi molecules as Multi-RNAi-NPs.

To address potential biomedical applications of our engineered platform, we further investigated the efficacy of the Multi-RNAi-NPs with respect to enzyme (Dicer) processing, cellular delivery, gene silencing, and cellular cytotoxicity (Figure S6). Dicer processing showed that the Multi-RNAi-MSs contained multiple polymeric RNAi molecules while retaining their biological capacity. Multi-RNAi-NPs (GFP-RFP-RNAi-MS/PEI) were transfected into cancer cells (HeLa cells), and the cellular uptake was analyzed. The Multi-RNAi-NPs were labeled with fluorescent Cy5-UTP (red) during the RCT process. Confocal microscopy images show that the Multi-RNAi-NPs were successfully delivered to cells (Figure 4D). This cellular uptake was attributed to endocytosis because no fluorescence was observed inside the

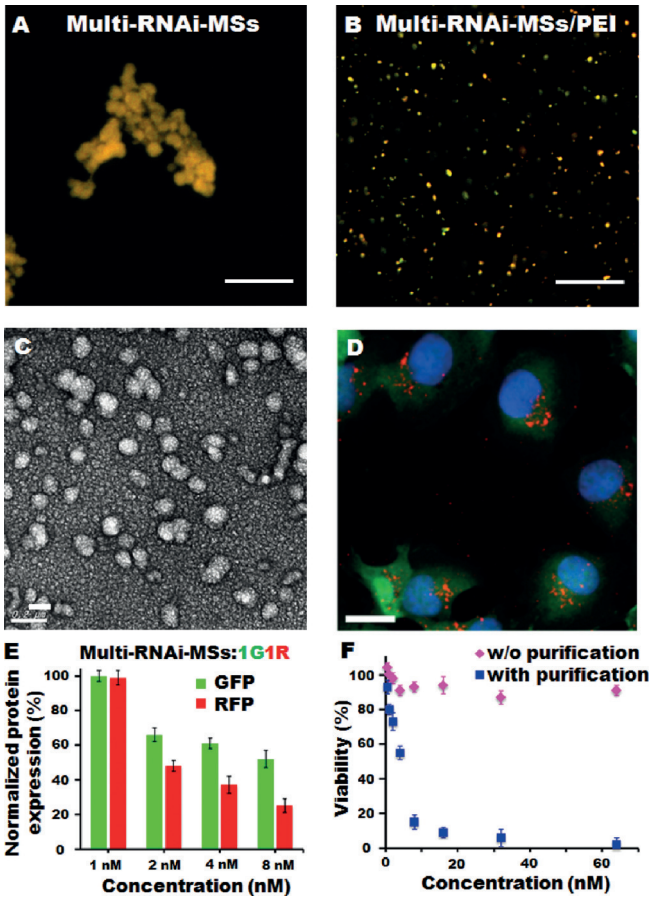

Figure 4. Characterization of Multi-RNAi-NPs after condensation. A,B) Confocal microscopy images confirming the co-localization of multiple polymeric RNAi molecules (corresponding to green and red fluorescence, respectively) within Multi-RNAi-MSs and Multi-RNAi-NPs. C) TEM image of the Multi-RNAi-NPs. D) Confocal microscopy image of HeLa cells treated with Multi-RNAi-NPs. The Multi-RNAi-NPs had been labeled with Cy5-conjugated UTP (red). The actin cytoskeleton was stained green with phalloidin, and the nucleus was stained blue with DAPI. Scale bar: 10 μm. E) The in vitro knockdown efficiency of GFP and RFP expression using PEI-condensed Multi-RNAi-MSs was examined as a function of concentration. F) The viability of cancer cells after 48 hours of incubation with Multi-RNAi-NPs was determined in MTT assays. The relative viabilities were assessed by comparing the signals of treated cells to those of non-treated control cells.

cells when endocytosis was inhibited by incubation at 4 °C (Figure S7). The Multi-RNAi-NP platform can be used to incorporate siRNAs targeting several mRNAs on the cellular level. As a proof of concept for the hypothesis that more than one gene can be silenced with Multi-RNAi-NPs, it was shown that HeLa cells that were engineered to stably overexpress GFP and RFP exhibited substantial target gene knockdown in a dose-dependent manner after the cellular uptake of Multi-RNAi-NPs. With a predefined combination ratio of 1:1 (the molar ratio between the two polymeric RNAi molecules in GFP-RFP-RNAi-MS/PEI), the GFP and RFP expression levels were silenced by (52 ± 5) % and (25 ± 4) %, respectively, at a concentration of 8 nM (Figure 4E). The viability of cancer cells at 48 h post-transfection with Multi-RNAi-NPs was subsequently measured by an MTT assay. Transfection with PEI-condensed Multi-RNAi-NPs was associated with much higher cell viabilities after removing the excess unincorporated PEI in a purification process following the condensation step (Figure 4F). It is notable that the knockdown increases with increasing concentrations for both the GFP and RFP RNAi sequences, indicating that the knockdown scales equally for both systems in these multi-RNAi sequences. Furthermore, all Multi-RNAi-MSs (i.e., 4G1R, 2G1R, 1G1R, 1G2R, and 1G4R) were evaluated for knockdown of the target mRNAs, indicating the ratio controllability of the in vitro knockdown with the Multi-RNAi-MSs system (Figure S8). Overall, the engineered Multi-RNAi-NPs were efficiently taken up by cells and facilitated efficient targeting of multiple genes, achieving silencing with negligible cytotoxicity.

In summary, the RCT generation of polymeric RNAi systems is versatile, and enables the production of polymeric RNAi for the silencing of multiple genes within the same RNAi-MS. We have developed a novel platform for efficiently packaging and delivering multiple RNAi molecules, which is thus capable of simultaneously regulating multiple biological functions. As the encoded RNA strands were easily modified by circular DNA template design, we could incorporate numerous polymeric RNAi molecules into a single Multi-RNAi-MS, expanding both their versatility and applicability. Using a combination of hybrid DNA templates, ratiometric composites of polymeric RNAi could be rationally engineered, allowing for precise control over the stoichiometry of the RNAi repeats. With an appropriate condensation method, the resulting nanosized delivery platform facilitated efficient RNAi in cancer cells. Our approach to efficiently package and simultaneously deliver multiple polymeric RNAi molecules could provide additive and synergistic effects for RNAi-based cancer therapy.

Acknowledgements

We gratefully acknowledge the funding of this work through a DoD OCRP Teal Innovator Award (OC120504). We thank the MIT Koch Institute Swanson Biotechnology Center, which is supported by the Koch Institute Core Grant P30-CA14051 from the NCI, for the use of facilities, specifically the microscopy and flow cytometry cores. This work was supported by the National Research Foundation of Korea (2015R1C1A1A02037770) and by the Yonsei University Future-leading Research Initiative of 2015 (2015-22-0085). This work was also supported by the National Institutes of Health (1F32EB017614-02 to E.C.D.).

Keywords: cancer · DNA/RNA nanotechnology · multifunctionality · RNA interference · siRNA delivery

How to cite: *Angew. Chem. Int. Ed.* **2016**, *55*, 3347–3351
Angew. Chem. **2016**, *128*, 3408–3412

[1] a) P. Guo, *Nat. Nanotechnol.* **2010**, *5*, 833–842; b) P. Guo, F. Haque, B. Hallahan, R. Reif, H. Li, *Nucleic Acid Ther.* **2012**, *22*, 226–245; c) C. J. Delebecque, A. B. Lindner, P. A. Silver, F. A.

Aldaye, *Science* **2011**, *333*, 470 – 474; d) B. Cayrol, C. Nogues, A. Dawid, I. Sagi, P. Silberzan, H. Isambert, *J. Am. Chem. Soc.* **2009**, *131*, 17270 – 17276; e) G. C. Shukla, F. Haque, Y. Tor, L. M. Wilhelmsson, J. J. Toulme, H. Isambert, P. Guo, J. J. Rossi, S. A. Tenenbaum, B. A. Shapiro, *ACS Nano* **2011**, *5*, 3405 – 3418.

[2] a) L. Jaeger, E. Westhof, N. B. Leontis, *Nucleic Acids Res.* **2001**, *29*, 455 – 463; b) A. Chworos, I. Severcan, A. Y. Koyfman, P. Weinkam, E. Oroudjev, H. G. Hansma, L. Jaeger, *Science* **2004**, *306*, 2068 – 2072; c) D. Shu, W. D. Moll, Z. X. Deng, C. D. Mao, P. X. Guo, *Nano Lett.* **2004**, *4*, 1717 – 1723; d) F. J. Isaacs, D. J. Dwyer, J. J. Collins, *Nat. Biotechnol.* **2006**, *24*, 545 – 554; e) I. Severcan, C. Geary, A. Chworos, N. Voss, E. Jacovetty, L. Jaeger, *Nat. Chem.* **2010**, *2*, 772 – 779.

[3] a) J. Soutschek, A. Akinc, B. Bramlage, K. Charisse, R. Constien, M. Donoghue, S. Elbashir, A. Geick, P. Hadwiger, J. Harborth, M. John, V. Kesavan, G. Lavine, R. K. Pandey, T. Racie, K. G. Rajeev, I. Rohl, I. Toudjarska, G. Wang, S. Wuschko, D. Bumcrot, V. Koteliansky, S. Limmer, M. Manoharan, H. P. Vornlocher, *Nature* **2004**, *432*, 173 – 178; b) J. H. Zhou, Y. Shu, P. X. Guo, D. D. Smith, J. J. Rossi, *Methods* **2011**, *54*, 284 – 294; c) S. K. Basu, *Hepatology* **2012**, *56*, 795a – 796a; d) E. Farjami, R. Campos, J. S. Nielsen, K. V. Gothelf, J. Kjems, E. E. Ferapontova, *Anal. Chem.* **2013**, *85*, 121 – 128; e) Y. Shu, F. Pi, A. Sharma, M. Rajabi, F. Haque, D. Shu, M. Leggas, B. M. Evers, P. Guo, *Adv. Drug Delivery Rev.* **2014**, *66*, 74 – 89; f) H. Li, T. Lee, T. Dziubla, F. Pi, S. Guo, J. Xu, C. Li, F. Haque, X.-J. Liang, P. Guo, *Nano Today* **2015**, *10*, 631 – 655.

[4] K. A. Whitehead, R. Langer, D. G. Anderson, *Nat. Rev. Drug Discovery* **2009**, *8*, 129 – 138.

[5] J. B. Lee, J. Hong, D. K. Bonner, Z. Poon, P. T. Hammond, *Nat. Mater.* **2012**, *11*, 316 – 322.

[6] K. E. Shopsowitz, Y. H. Roh, Z. J. Deng, S. W. Morton, P. T. Hammond, *Small* **2014**, *10*, 1623 – 1633.

[7] Y. H. Roh, J. B. Lee, K. E. Shopsowitz, E. C. Dreaden, S. W. Morton, Z. Poon, J. Hong, I. Yamin, D. K. Bonner, P. T. Hammond, *ACS Nano* **2014**, *8*, 9767-80.

[8] a) A. Khaled, S. C. Guo, F. Li, P. X. Guo, *Nano Lett.* **2005**, *5*, 1797 – 1808; b) P. K. Chandra, A. K. Kundu, S. Hazari, S. Chandra, L. L. Bao, T. Ooms, G. F. Morris, T. Wu, T. K. Mandel, S. Dash, *Mol. Ther.* **2012**, *20*, 1724 – 1736; c) W. Hasan, K. Chu, A. Gullapalli, S. S. Dunn, E. M. Enlow, J. C. Luft, S. M. Tian, M. E. Napier, P. D. Pohlhaus, J. P. Rolland, J. M. DeSimone, *Nano Lett.* **2012**, *12*, 287 – 292; d) J. E. Dahlman, C. Barnes, O. F. Khan, A. Thiriot, S. Jhunjunwala, T. E. Shaw, Y. P. Xing, H. B. Sager, G. Sahay, L. Speciner, A. Bader, R. L. Bogorad, H. Yin, T. Racie, Y. Z. Dong, S. Jiang, D. Seedorf, A. Dave, K. S. Sandhu, M. J. Webber, T. Novobrantseva, V. M. Ruda, A. K. R. Lytton-Jean, C. G. Levins, B. Kalish, D. K. Mudge, M. Perez, L. Abezgauz, P. Dutta, L. Smith, K. Charisse, M. W. Kieran, K. Fitzgerald, M. Nahrendorf, D. Danino, R. M. Tuder, U. H. von Andrian, A. Akinc, D. Panigrahy, A. Schroeder, V. Koteliansky, R. Langer, D. G. Anderson, *Nat. Nanotechnol.* **2014**, *9*, 648 – 655.

[9] a) Z. Medarova, W. Pham, C. Farrar, V. Petkova, A. Moore, *Nat. Med.* **2007**, *13*, 372 – 377; b) S. D. Li, Y. C. Chen, M. J. Hackett, L. Huang, *Mol. Ther.* **2008**, *16*, 163 – 169; c) A. Elbakry, A. Zaky, R. Liebkl, R. Rachel, A. Goepferich, M. Breunig, *Nano Lett.* **2009**, *9*, 2059 – 2064; d) H. Lee, A. K. R. Lytton-Jean, Y. Chen, K. T. Love, A. I. Park, E. D. Karagiannis, A. Sehgal, W. Querbes, C. S. Zurenko, M. Jayaraman, C. G. Peng, K. Charisse, A. Borodovsky, M. Manoharan, J. S. Donahoe, J. Truelove, M. Nahrendorf, R. Langer, D. G. Anderson, *Nat. Nanotechnol.* **2012**, *7*, 389 – 393; e) Z. J. Deng, S. W. Morton, E. Ben-Akiva, E. C. Dreaden, K. E. Shopsowitz, P. T. Hammond, *ACS Nano* **2013**, *7*, 9571 – 9584.

[10] A. Albanese, P. S. Tang, W. C. W. Chan, *Annu. Rev. Biomed. Eng.* **2012**, *14*, 1 – 16.

Received: September 24, 2015
Revised: November 4, 2015
Published online: December 22, 2015

